coatings

MDPI

*Article*

# Microstructure and Properties in Simulated Seawater of Copper-Doped Micro-arc Coatings on TC4 Alloy

**Yong Zhang [1], Wei Yang [1,*], Sen Yu [2], Liqun Wang [3], Xiqun Ma [2], Wei Gao [1], Nan Lan [1], Wenting Shao [1] and Jian Chen [1]**

[1] School of Materials Science and Chemical Engineering, Xi'an Technological University, Xi'an 710021, China; zhangyong@st.xatu.edu.cn (Y.Z.); gaowei@xatu.edu.cn (W.G.); 15082383495@163.com (N.L.); wentingshao@xatu.edu.cn (W.S.); chenjian@xatu.edu.cn (J.C.)
[2] Shaanxi Key Laboratory of Biomedical Metal Materials, Northwest Institute for Non-ferrous Metal Research, Xi'an 710016, China; ninbrc@163.com (S.Y.); maxiqun23@126.com (X.M.)
[3] School of Materials Science and Engineering, Xi'an Jiaotong University, Xi'an 710049, China; wanglq@mail.xjtu.edu.cn
* Correspondence: yangwei_smx@163.com; Tel./Fax: +86-029-8617-3324

**Abstract:** Micro-arc oxidation (MAO) ceramic coatings were prepared on TC4 titanium alloys by adding $CuSO_4$ to a $(NaPO_3)_6$ base solution. The microstructures of the MAO coatings were characterized by scanning electron microscopy (SEM), energy dispersive (EDS), and X-ray photoelectron spectroscopy (XPS). The corrosion resistance and wear resistance of these coatings were evaluated via hydrochloric acid immersion of weight deficit and friction tests. Those results indicated the presence of Cu in the MAO coating in the form of CuO and $Cu_2O$. Incorporation of $CuSO_4$ results in a thickness and roughness increase in the coating. The coating has a lower coefficient of friction (0.2) upon the addition of 4 g/L of $CuSO_4$. The antibacterial properties of the MAO coatings were maximized at 6 g/L of $CuSO_4$. However, the corrosion resistance of the copper-doped MAO coating did not exceed the undoped coating. This study shows that the addition of $CuSO_4$ to the electrolyte successfully prepared copper-containing micro-arc oxidation coatings, which improved the wear resistance and antibacterial properties of the coating.

**Keywords:** titanium alloy; micro-arc oxidation; coating; microstructure; properties



**Citation:** Zhang, Y.; Yang, W.; Yu, S.; Wang, L.; Ma, X.; Gao, W.; Lan, N.; Shao, W.; Chen, J. Microstructure and Properties in Simulated Seawater of Copper-Doped Micro-arc Coatings on TC4 Alloy. *Coatings* **2022**, *12*, 883. https://doi.org/10.3390/coatings12070883

Academic Editor: Stefano Caporali

Received: 13 May 2022
Accepted: 7 June 2022
Published: 22 June 2022



## 1. Introduction

Titanium and titanium alloys have been widely used in aerospace engineering, marine engineering, biomedicine, and many other fields due to their high specific strength, lightweight, low-temperature resistance, and good biocompatibility [1–4]. In marine engineering, titanium and its alloys have become indispensable materials in this field. However, titanium and its alloys also have disadvantages, such as low hardness, easy marine organism adhesion, and poor corrosion resistance [5,6]. Therefore, current challenges for material scientists include improving the corrosion resistance and tribological performance of titanium alloys. Various surface modifications, low friction, and corrosion-resistant coatings have been advanced to address this problem. The protective coatings significantly improved titanium alloy performances involving friction and wear [7].

Micro-arc oxidation (MAO) generates a ceramic oxide coating containing a base metal alloy with a porous structure and good valve metal adhesion (Ti, Mg, and Al) through arc discharge. In addition, MAO technology is simple, environmentally friendly, and applicable at higher external voltages compared with conventional anodizing [8,9]. Micro-arc discharge promotes molten oxide injection, which cools rapidly after contact with an electrolyte, and promotes the growth of ceramic coatings and oxide deposition [9]. The electrolyte composition often influences the MAO coating composition. Therefore,

MAO coating performances improve upon additive (such as Cu, Ag) introduction into the electrolyte [10,11].

Copper and its oxides have good wear reduction and antibacterial properties, and the addition of copper to MAO coatings has improved their protective and anti-fouling properties [12,13]. Multiple Cu sources, such as Cu nanoparticles [14], $Cu(C_6H_{11}O_7)_2$ [15], $Cu(CH_3COO)_2$ [16], and $Cu(NO_3)_2$ [17] were added to the electrolyte, and MAO coatings containing copper were successfully fabricated on a titanium alloy. However, the introduction of copper also causes a certain degree of degradation of the original corrosion resistance of the coating [18]. For example, He et al. [19] successfully prepared black MAO coatings on magnesium alloys by introducing copper into the electrolyte, and the increase in copper content eventually led to a decrease in the corrosion resistance of the coatings. Previously, we reported the effects of copper pyrophosphate on the structure and properties of TC4 micro-arc oxide coatings [20]. CuSO4 has been extensively used in industry as an insecticide and antibacterial agent. Furthermore, to illustrate the effect of different metal salt concentrations on the structure and properties of micro-arc oxidation coatings, we used copper sulfate to investigate the concentration effect on the coating.

A protective coating was prepared on the TC4 alloy by altering $CuSO_4$ concentrations in the electrolyte by MAO technology to improve the shortcomings of titanium alloy in a marine environment. The effects of $CuSO_4$ on the morphology, composition, corrosion resistance, wear resistance, and antibacterial properties of MAO coating were studied, and an optimized $CuSO_4$ concentration was obtained to improve the properties of the MAO coating.

## 2. Experimental

### *2.1. Material Preparation*

TC4 alloy, with a size of φ 20 mm × 4 mm, was used as the substrate material. The samples were ground and polished with 400#, 600#, 800#, 1000#, 1200#, and 1500# sand paper to obtain a smooth surface, then sonicated in ethanol for 20 min, deionized water for 10 min, and dried in air. The basic MAO electrolyte was 20 g/L $(NaPO_3)_6$ + 3 g/L $Na_2WO_4$ + 3 g/L KF + 4 g/L KOH. Copper sulfate was added to the electrolyte solution (0, 2, 4, 6, 8, and 10 g/L $CuSO_4$). Sodium citrate was added to complex the $Cu^{2+}$, and thus the complex ions were negatively charged. This enhanced the doping efficiency relative to the conventional neutral and positively charged Cu sources by facilitating electromigration to the anode under an electric field during micro-arc oxidation [20]. Under a constant voltage of 450 V, frequency 600 Hz, and a duty cycle of 3%, the MAO treatment lasted 15 min. The electrolyte temperature needs to be maintained at 20–40 °C during the preparation of the MAO coating.

### *2.2. Structure and Performance Characterization*

The surface morphology of MAO coatings was observed and analyzed by SEM (TESCAN VEGA 3-SBH, Shanghai Taseken Trading Company, magnification 1000×, work distance 10 mm, resolution 30 KV). X-ray photoelectron spectroscopy (Shimadzu-Kratos Co. Ltd., Hadano, Japan) examined the surface chemical state of the MAO coating. The elemental distribution in the coating and wear marks were analyzed by EDS (TESCAN VEGA 3-SBH, Shanghai Taseken Trading Company, Shanghai, China); a TT260 (Beijing Times, Beijing, China) eddy current thickness gauge characterized the thickness and roughness of the MAO coating. The friction and wear of the substrate and MAO coating were tested in simulated seawater using an HT-1000 (Zhongke Kaihua Technology Development Co. LTD, Lanzhou, China) friction and wear tester. The wear material was GCr15, the test load was 500 g, the rotating speed was 280 r/min, and the friction radius was 3 mm.

The MAO coating specimens prepared by adding different concentrations of $CuSO_4$ were immersed in a 1 M hydrochloric acid solution. The corrosion resistance of the coatings was evaluated by weighing them every 2 days, totaling the weight loss after 10 days. Then, *Staphylococcus aureus* was poured into the sterilized culture medium, cultured on a constant

temperature via shaking the table for 24 h, and the cultured bacterial solution was washed and redispersed into normal saline. After sample sterilization and cleaning upon micro-arc oxidation, the samples were placed in a 12-well plate, and an aliquot 1500 μL of bacterial solution was added to the surface of each sample. The optical density (OD) was measured after incubation at constant temperature and shaking at 37 °C for 3 days. The bacteria not attached to the sample surface were cleaned, and bacterial adhesions on the surfaces with different $CuSO_4$ concentrations were observed by SEM.

## 3. Results and Discussion

Figure 1 shows the surface morphologies of the MAO coating prepared by adding different concentrations of $CuSO_4$. The MAO coating shows "volcano crater" porous features. The addition of $CuSO_4$ increases the electrical conductivity of the solution, which increases the current density at the specimen surface and generates more heat at the reaction interface; this promotes oxide melting and solidification. As a result, there was a discontinuous oxide distribution on the MAO coating; however, the addition of 6 g/L $CuSO_4$ resulted in a smooth and flat MAO coating with few bumps. With added $CuSO_4$, the micro-pores on the coating increased slightly, a result of the interconnection between smaller diameter micro-pores due to a solution conductivity increase.

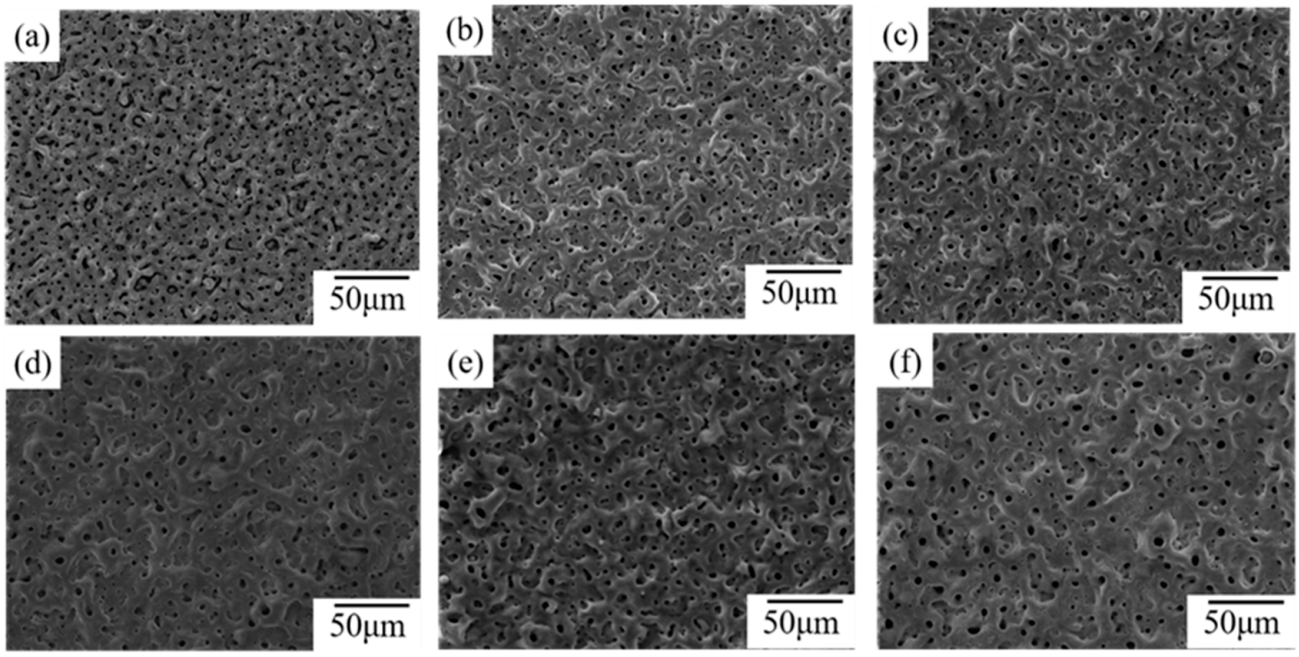


**Figure 1.** Surface microstructure of MAO coating prepared at different electrolytes with the addition of $CuSO_4$ of (**a**) 0, (**b**) 2, (**c**) 4, (**d**) 6, (**e**) 8, and (**f**) 10 g/L.

As shown in Figure 2, there was a positive correlation with the added copper sulfate. The initial thickness of the coating without the addition of $CuSO_4$ was only 6.24 μm. At $CuSO_4$ concentrations between 4–6 g/L, the thickness change was not very clear (~22 μm). As the concentration increased from 6 to 8 g/L, the roughness coating increased significantly, and its thickness maximized at 22.94 μm. The $Cu^{2+}$ concentration increase led directly to a solution conductivity increase, which led to similar increases in the thickness and roughness of the coating [20]. According to XPS results, Cu entered the MAO coating, which explains the thickening of the coating [21].

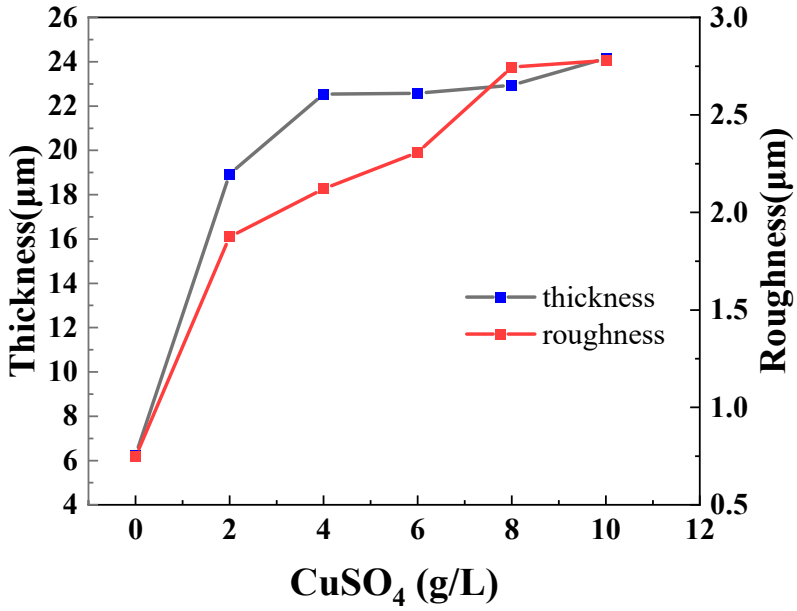


**Figure 2.** Thickness and roughness of MAO coating with different concentrations of $CuSO_4$.

The surface of the MAO coating was explored by XPS to investigate the elemental chemical states in the coating, especially Cu. The XPS survey spectrum of the coating is shown in Figure 3a, which indicates the presence of Ti, P, and Cu on the surface. The high-resolution XPS spectrum of Cu 2p is shown in Figure 3b, and contains four deconvoluted peaks located at 932.7 eV (2p3/2) and 952.4 eV (2p1/2) for $Cu_2O$, 934.5 eV (2p3/2) and 955.0 eV (2p1/2) for CuO [22]. This indicated that both $Cu_2O$ and CuO were present in the coating. The high-resolution XPS spectrum of Ti 2p is shown in Figure 3c. The binding energies of Ti 2p peaks at 458.6 and 464.7 eV confirm that titanium is present as $TiO_2$ [18]. The P 2p spectra revealed the expected doublet with P 2p3/2 at 133.0 eV and P 2p1/2 at 134.4 eV, which correspond to the binding energies of isolated P-O tetrahedra and polyphosphates, respectively [23]. XPS analysis showed that the micro discharge resulted in complex ionization, which formed $Cu_2O$ and CuO [24]. The XPS results illustrated that the friction coefficient of the coating can be reduced by successful incorporation of Cu into the coating, which agreed with friction experiment results. In addition, CuO formed, which improved the antimicrobial properties of the coating [22]. For MAO treatment, titanium is served as the anode. Therefore, during MAO, reaction 1 took place. Through the reaction, free electrons were developed. At the same time, copper hydroxide is generated as an oxide by the thermal dehydration reaction, in which the copper hydroxide that obtains free electrons generated by hydroxide discharge generates cuprous oxide [25,26]. The reaction equations involved have been listed as follows:

$$Ti \rightarrow Ti^{4+} + 4e^- \quad (1)$$

$$Cu^{2+} + 2OH^- \rightarrow Cu(OH)_2 \quad (2)$$

$$Cu(OH)_2 \rightarrow 2CuO + H_2O \quad (3)$$

$$2Cu(OH)_2 + 2e^- \rightarrow Cu_2O + H_2O + 2OH^- \quad (4)$$

Figure 4 shows the change curves of the MAO coating friction coefficients at different $CuSO_4$ concentrations in the simulated seawater. At the beginning of the wear period, the friction coefficients of coatings with different $CuSO_4$ concentrations rose by different degrees and gradually leveled off as the friction time increased. This was due to the uneven "crater" shape of the coating surface, which has a high resistance when the abrasive ball initiates contact with the coating [27]. Abrasive chips accumulated into the coating

micro-pores with time, which resulted in a reduction in the friction coefficient. In the absence of $CuSO_4$, the friction coefficient was high, but the addition of $CuSO_4$ lowered it significantly. The coefficient of friction minimized when the $CuSO_4$ concentration was 4 g/L and increased with additional copper sulfate. This was due to Cu incorporation into the coating, although the self-lubricating effect of copper reduced the coating friction coefficient, Cu is a soft phase compared with the ceramic phase. Therefore, introducing a large amount of copper lowers the coating hardness, thus the friction coefficient increases. The mutual competition between the two explains why the coating friction coefficient shows a parabolic change. In addition, upon $CuSO_4$ addition of 4 and 6 g/L, the friction coefficients were similar, though minimalized. SEM showed that the surface coating was flat and without large bumps; the diameters and micro-pores were relatively small, which is considered as the best self-lubrication effect of Cu at this concentration.

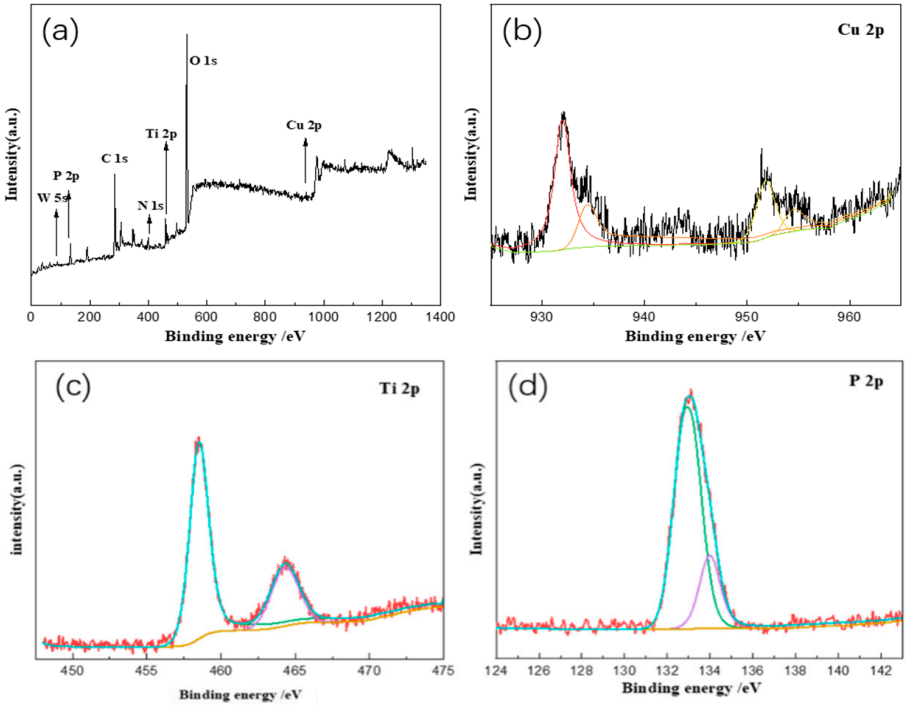


**Figure 3.** XPS spectra of MAO coating: (**a**) Survey; (**b**) Cu; (**c**) Ti; and (**d**) P.

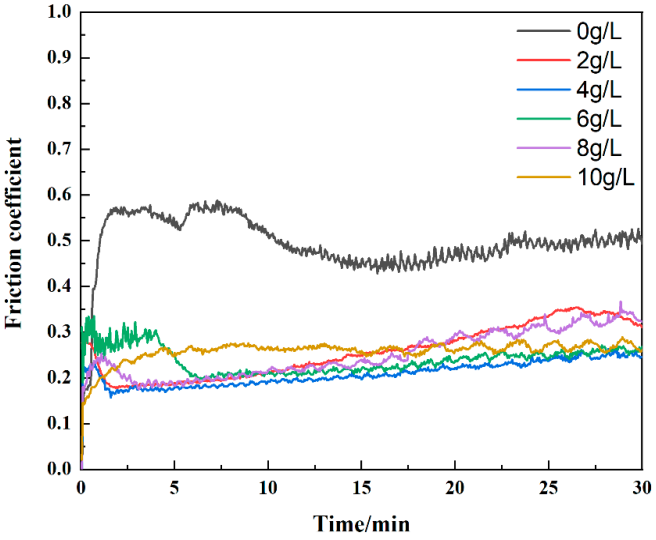


**Figure 4.** Wear curves of MAO-treated titanium alloys doped with $CuSO_4$ at various concentrations.

Figure 5 shows the SEM morphologies and EDS results of the MAO coating with different $CuSO_4$ concentrations added in seawater simulations. The MAO coating surface morphology with added $CuSO_4$ is flatter and smoother than without $CuSO_4$ addition [28]. This was due to the MAO surface coating formed by the addition of excessive $CuSO_4$; this introduced more bumps during coating and the grinding ball. They shed those to form abrasive particles and filled the coating micro-pore, which resulted in the wear coating surface gradually becoming tight, flat, and smooth as compared with the non-wear, whose coating surface hardness may increase. This further improves the wear resistance of the coating. Wear without the addition of the $CuSO_4$ MAO coating not only smooths out the surface micro-porosity, but enriches Fe and a relative reduction of elemental Ti at the wear marks. This is probably due to the cutting effect of the MAO coating surface projection on the grinding ball during wear. In addition, the abrasion mark widths after wear of the MAO coating decreased, while the $CuSO_4$ concentration increased, due to additional Cu in the MAO coating. This gives the coating a more clear self-lubrication. At the same time, EDS results indicated that the amount of O was higher at the abrasion marks than in the unworn areas, due to the frictional heat during micro-pore filling by the abrasive chips of the grinding balls during wear. This was due to oxidation that occurred during the filling of the micro-pores by frictional heat.

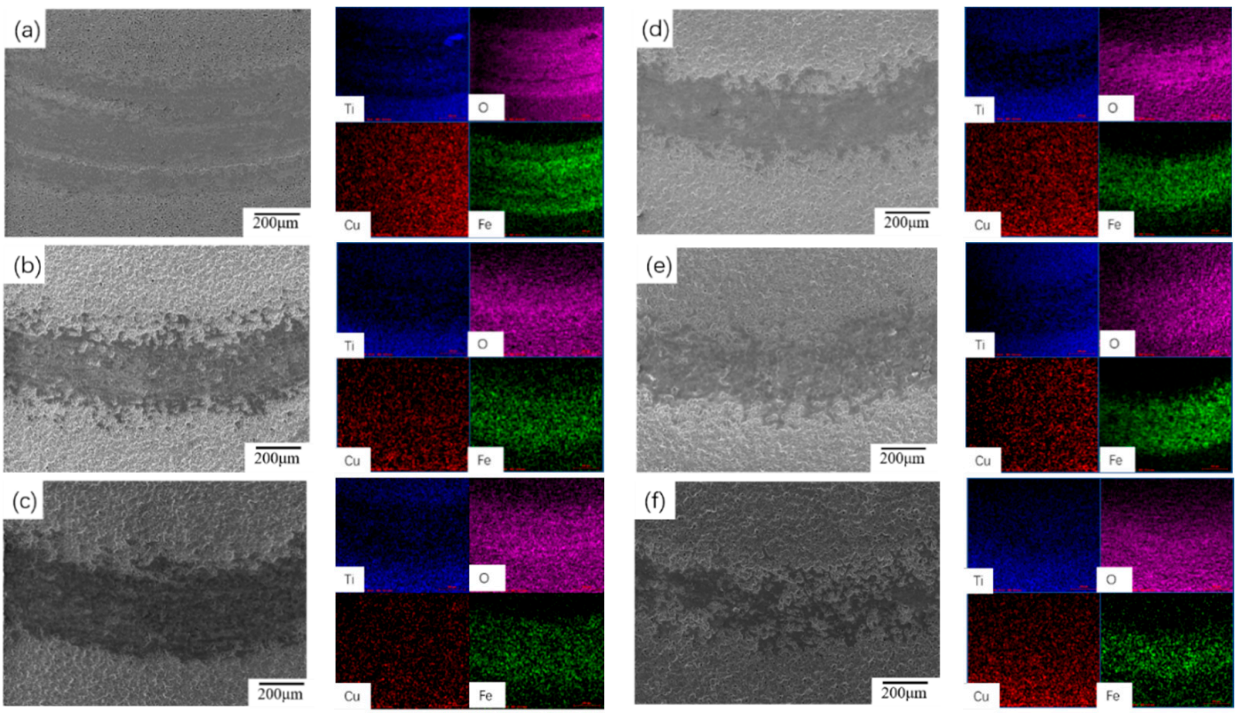


**Figure 5.** SEM images and EDS spectrums of MAO-treated TC4 with various concentrations of $CuSO_4$ doping: (**a**) 0, (**b**) 2, (**c**) 4, (**d**) 6, (**e**) 8, and (**f**) 10 g/L.

The corrosion resistance of MAO coating formed in electrolytes with various $CuSO_4$ concentrations was tested in 1 mol/L HCl solutions at room temperature via weight loss, as shown in Figure 6. The MAO coating with different $CuSO_4$ additions had negative corrosion resistance compared with the MAO coating without $CuSO_4$ addition. This result indicated that the corrosion resistance decreased [29]. Increasing concentrations of $CuSO_4$ increased the amount of Cu doped into the MAO coating, which decreased the corrosion resistance. Furthermore, the addition of $CuSO_4$ to the surface morphology of MAO coating (optimized at 6 g/L $CuSO_4$) resulted in smooth surface features that improved corrosion resistance.

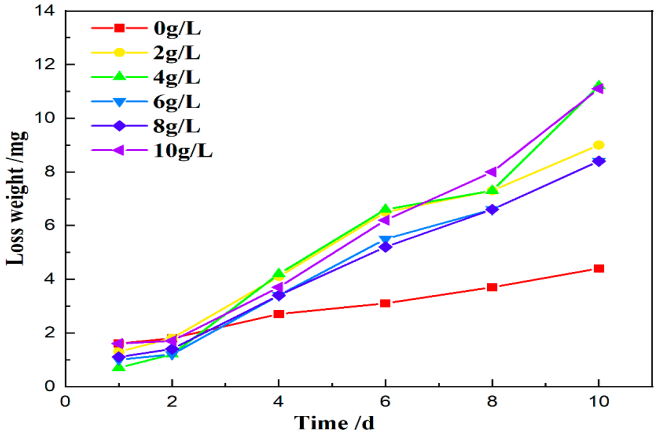


**Figure 6.** Hydrochloric acid immersion weight loss curves of MAO coating with the addition of various concentrations of $CuSO_4$.

Figure 7 shows the SEM of *S. aureus* after Figure 3d incubation in the micro-arc oxide coating prepared by adding different concentrations of $CuSO_4$. *S. aureus* aggregates at the discharge channel of the membrane coating. Upon $CuSO_4$ addition, bacteria attached to the surface of the MAO coating decreased significantly and weakened the aggregation state. This was due to a clear inhibitory effect of copper and its oxides on bacterial growth [30]. The addition of $CuSO_4$ at 6 g/L minimized the number of bacteria on the coating; additional $CuSO_4$ did not significantly impact the number of bacteria on the surface. The best inhibition effect on *S. aureus* was achieved when the electrolyte $CuSO_4$ concentration was 6 g/L. Table 1 shows the OD values of the micro-arc oxidation coating with different concentrations of $CuSO_4$. The incorporation of Cu significantly reduced the OD and enhanced the antibacterial and bactericidal performances of the coating. The OD value minimized when the $CuSO_4$ concentration in the electrolyte was 6 g/L and agreed with SEM results.

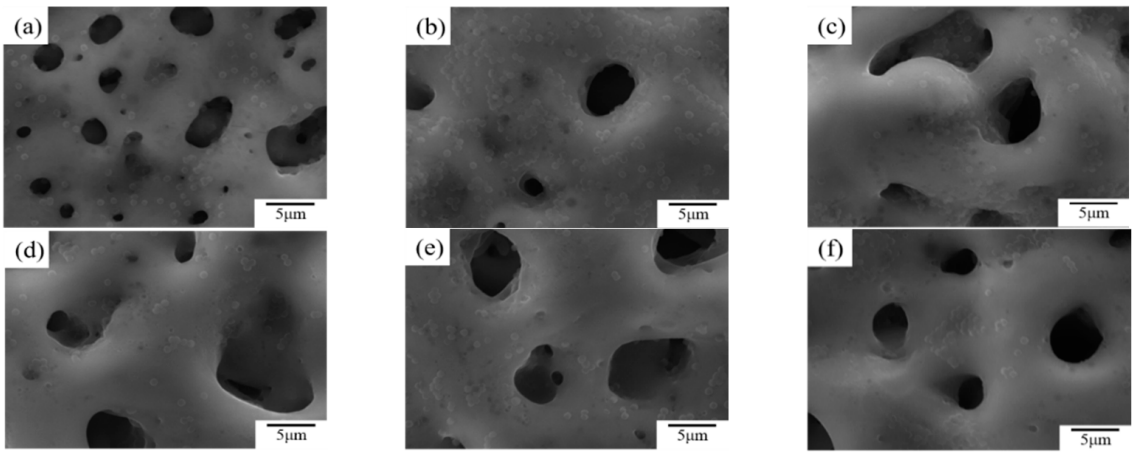


**Figure 7.** Bacterial adhesion morphologies of MAO coating with different $CuSO_4$ additions of (**a**) 0, (**b**) 2, (**c**) 4, (**d**) 6, (**e**) 8, and (**f**) 10 g/L.

**Table 1.** OD values of $CuSO_4$ specimens added at different concentrations in a constant temperature shaker for 3 days.

| Samples | S0 | S2 | S4 | S6 | S8 | S10 | Saline |
|---|---|---|---|---|---|---|---|
| **OD value** | 1.160 | 0.834 | 0.792 | 0.526 | 0.546 | 0.559 | 0.500 |

## 4. Conclusions

(1) Incorporation of $CuSO_4$ significantly improved the surface morphology of the MAO coating and enhanced the coating thickness; a concentration of 6 g/L unified the surface morphology of the coating and minimized the number and diameter of micro-pores.

(2) The addition of $CuSO_4$ significantly reduced the friction coefficient of the coating. As the concentration of $CuSO_4$ increased, the friction coefficient fluctuation decreased, the width of the abrasion marks decreased, and the wear dopped. The MAO coating with 4 g/L $CuSO_4$ had excellent wear resistance with a small friction coefficient of 0.2.

(3) The addition of $CuSO_4$ lowered the corrosion resistance of the coating. However, there was a significant inhibitory effect on the proliferation of *S. aureus*, and the number of bacteria attached to the surface of the coating was significantly reduced, with a minimum OD value of 0.526 at a $CuSO_4$ concentration of 6 g/L.

**Author Contributions:** Conceptualization, methodology, and writing—original draft preparation, Y.Z. and W.Y.; writing—review and editing, S.Y., N.L., L.W., W.S., X.M. and W.G.; supervision, J.C. All authors have read and agreed to the published version of the manuscript.

**Funding:** This work was financially supported by the National Natural Science Foundation of China (No. 52071252), China Postdoctoral Science Foundation (No. 2020M683670XB), Scientific Research Program funded by Shaanxi Provincial Education Department (No. 21JP053), and Key research and development plan of Shaanxi Province Industrial Project (2021GY-208, 2022GY-407, and 2021ZDLSF03-11).

**Institutional Review Board Statement:** Not applicable.

**Informed Consent Statement:** Not applicable.

**Conflicts of Interest:** The authors declare no conflict of interest.

## References

1. Lu, J.; Zhang, Y.; Huo, W.; Zhang, W.; Zhao, Y.; Zhang, Y. Electrochemical corrosion characteristics and biocompatibility of nanostructured titanium for implants. *Appl. Surf. Sci.* **2018**, *434*, 63–72. [CrossRef]
2. Zhang, L.; Gao, Q.; Han, Y. Zn and Ag Co-doped Anti-microbial $TiO_2$ Coatings on Ti by Micro-arc Oxidation. *J. Mater. Sci. Technol.* **2016**, *32*, 919–924. [CrossRef]
3. Zhu, J.; Jia, H.; Liao, K.; Li, X. Improvement on corrosion resistance of micro-arc oxidized AZ91D magnesium alloy by a pore-sealing coating. *J. Alloys Compd.* **2022**, *889*, 161460. [CrossRef]
4. Yang, W.; Gao, Y.; Xu, D.; Zhao, J.; Ke, P.; Wang, A. Bactericidal abilities and in vitro properties of diamond-like carbon films deposited onto MAO-treated titanium. *Mater. Lett.* **2019**, *244*, 155–158. [CrossRef]
5. Ren, S.; Du, C.; Liu, Z.; Li, X.; Xiong, J.; Li, S. Effect of fluoride ions on corrosion behaviour of commercial pure titanium in artificial seawater environment. *Appl. Surf. Sci.* **2020**, *506*, 144759. [CrossRef]
6. Fazel, M.; Salimijazi, H.R.; Shamanian, M. Improvement of Corrosion and Tribocorrosion Behavior of Pure Titanium by Subzero Anodic Spark Oxidation. *ACS Appl. Mater. Interfaces* **2018**, *10*, 15281–15287. [CrossRef]
7. Huang, M.; Wang, Y.; Chu, C.-H.; Zhang, M.-X.; Wang, H.-B.; Xue, S.-X. Wear resistance of alumina-coated oil casing steel N80 via MAO with rare earth additive. *Ceram. Int.* **2017**, *43*, 6397–6402. [CrossRef]
8. Wang, Y.; Yu, H.; Chen, C.; Zhao, Z. Review of the biocompatibility of micro-arc oxidation coated titanium alloys. *Mater. Des.* **2015**, *85*, 640–652. [CrossRef]
9. Gao, A.; Hang, R.; Bai, L.; Tang, B.; Chu, P.K. Electrochemical surface engineering of titanium-based alloys for biomedical application. *Electrochim. Acta* **2018**, *271*, 699–718. [CrossRef]
10. Zhang, X.; Lu, X.; Lv, Y.; Yang, L.; Zhang, E.; Dong, Z. Enhancement of Corrosion Resistance and Biological Performances of Cu-Incorporated Hydrox-yapatite/$TiO_2$ Coating by Adjusting Cu Chemical Configuration and Hydroxyapatite Contents. *ACS Appl. Bio Mater.* **2021**, *4*, 903–917. [CrossRef]
11. Aydogan, D.T.; Muhaffel, F.; Acar, O.K.; Topcuoglu, E.N.; Kulekci, H.G.; Kose, G.T.; Baydogan, M.; Cimenoglu, H. Surface modification of Ti6Al4V by micro-arc oxidation in $AgC_2H_3O_2$-containing electrolyte. *Surf. Innov.* **2018**, *6*, 277–285. [CrossRef]
12. Jacobs, A.; Renaudin, G.; Forestier, C.; Nedelec, J.-M.; Descamps, S. Biological properties of copper-doped biomaterials for orthopedic applications: A review of antibacterial, angiogenic and osteogenic aspects. *Acta Biomater.* **2020**, *117*, 21–39. [CrossRef] [PubMed]
13. Liu, R.; Memarzadeh, K.; Chang, B.; Zhang, Y.; Ma, Z.; Allaker, R.P.; Ren, L.; Yang, K. Antibacterial effect of copper-bearing titanium alloy (Ti-Cu) against Streptococcus mutans and Porphyromonas gingivalis. *Sci. Rep.* **2016**, *6*, 29985. [CrossRef]

14. Yao, X.; Zhang, X.; Wu, H.; Tian, L.; Ma, Y.; Tang, B. Microstructure and antibacterial properties of Cu-doped $TiO_2$ coating on titanium by micro-arc oxidation. *Appl. Surf. Sci.* **2014**, *292*, 944–947. [CrossRef]
15. Zhao, Q.; Yi, L.; Hu, A.; Jiang, L.; Hong, L.; Dong, J. Antibacterial and osteogenic activity of a multifunctional microporous coating codoped with Mg, Cu and F on titanium. *J. Mater. Chem. B* **2019**, *7*, 2284–2299. [CrossRef] [PubMed]
16. Zhang, L.; Guo, J.; Yan, T.; Han, Y. Fibroblast responses and antibacterial activity of Cu and Zn co-doped $TiO_2$ for percutaneous implants. *Appl. Surf. Sci.* **2018**, *434*, 633–642. [CrossRef]
17. Rokosz, K.; Hryniewicz, T.; Kacalak, W.; Tandecka, K.; Raaen, S.; Gaiaschi, S.; Chapon, P.; Malorny, W.; Matýsek, D.; Dudek, L.; et al. Characterization of porous phosphate coatings enriched with calcium, magnesium, zinc and copper created on CP titanium grade 2 by plasma electrolytic oxidation. *Metals* **2018**, *8*, 411. [CrossRef]
18. Zhang, X.; Zhang, T.; Lv, Y.; Zhang, Y.; Lu, X.; Xiao, J.; Ma, C.; Li, Z.; Dong, Z. Enhanced uniformity, corrosion resistance and biological performance of Cu-incorporated $TiO_2$ coating produced by ultrasound-auxiliary micro-arc oxidation. *Appl. Surf. Sci.* **2021**, *569*, 150932. [CrossRef]
19. He, R.; Wang, B.; Xiang, J.; Pan, T. Effect of copper additive on microstructure and anti-corrosion performance of black MAO films grown on AZ91 alloy and coloration mechanism. *J. Alloys Compd.* **2021**, *889*, 161501. [CrossRef]
20. Gao, W.; Liu, J.; Wei, J.; Yao, Y.; Ma, X.; Yang, W. Enhanced properties of micro arc oxidation coating with Cu addition on TC4 alloy in marine environment. *Coatings* **2021**, *11*, 1168. [CrossRef]
21. Li, Q.; Zhao, M.; Li, L.; Dong, L.; Wu, J.; Li, D. Co-regulation of Cu/Zn contents enhanced the biological and mechanical properties of TiN coated Ti-6Al-4V alloy. *Surf. Coat. Technol.* **2020**, *395*, 125943. [CrossRef]
22. Zhang, X.; Peng, Z.; Lu, X.; Lv, Y.; Cai, G.; Yang, L.; Dong, Z. Microstructural evolution and biological performance of Cu-incorporated $TiO_2$ coating fabricated through one-step micro-arc oxidation. *Appl. Surf. Sci.* **2020**, *508*, 144766. [CrossRef]
23. Schreckenbach, J.P.; Marx, G.; Schlottig, F.; Textor, M.; Spencer, N.D. Characterization of anodic spark-converted titanium surfaces for biomedical applications. *J. Mater. Sci. Mater. Med.* **1999**, *10*, 453–457. [CrossRef] [PubMed]
24. Kamil, M.P.; Kaseem, M.; Ko, Y.G. Soft plasma electrolysis with complex ions for optimizing electrochemical performance. *Sci. Rep.* **2017**, *7*, srep44458. [CrossRef]
25. Wang, Y.; Zhao, S.; Li, G.; Zhang, S.; Zhao, R.; Dong, A.; Zhang, R. Preparation and in vitro antibacterial properties of anodic coatings co-doped with Cu, Zn, and P on a Ti-6Al-4V alloy. *Mater. Chem. Phys.* **2020**, *241*, 122360. [CrossRef]
26. Liang, T.; Wang, Y.; Zeng, L.; Liu, Y.; Qiao, L.; Zhang, S.; Zhao, R.; Li, G.; Zhang, R.; Xiang, J.; et al. Copper-doped 3D porous coating developed on Ti-6Al-4V alloys and its in vitro long-term antibacterial ability. *Appl. Surf. Sci.* **2020**, *509*, 144717. [CrossRef]
27. Chen, L.; Jin, X.; Qu, Y.; Wei, K.; Zhang, Y.; Liao, B.; Xue, W. High temperature tribological behavior of microarc oxidation film on Ti-39Nb-6Zr alloy. *Surf. Coat. Technol.* **2018**, *347*, 29–37. [CrossRef]
28. Lan, N.; Yang, W.; Gao, W.; Guo, P.; Zhao, C.; Chen, J. Characterization of ta-C film on micro arc oxidation coated titanium alloy in simulated seawater. *Diam. Relat. Mater.* **2021**, *117*, 108483. [CrossRef]
29. Zhang, C.; Zhang, F.; Song, L.; Zeng, R.; Li, S.; Han, E. Corrosion resistance of a superhydrophobic surface on micro-arc oxidation coated Mg-Li-Ca alloy. *J. Alloys Compd.* **2017**, *728*, 815–826. [CrossRef]
30. Yan, X.; Zhao, M.C.; Yang, Y.; Tan, L.; Zhao, Y.C.; Yin, D.F.; Yang, K.; Atrens, A. Improvement of biodegradable and antibacterial properties by solution treatment and mi-cro-arc oxidation (MAO) of a magnesium alloy with a trace of copper. *Corros. Sci.* **2019**, *156*, 125–138. [CrossRef]